NMR 2008

10th National Norwegian NMR Meeting
Oppdal, Norway, 16-18 January 2008

PROGRAM AND ABSTRACTS

Welcome to the 10th National Norwegian NMR Meeting

Recent advances in the field on Nuclear Magnetic Resonance (NMR) spectroscopy continue to make this technique indispensable for basic research, clinical tests and for its application in almost all branches of industry. Indeed, applications of NMR spectroscopy were reported for chemistry research, structural proteomics studies, various applications in food, pharmaceutical, petroleum industries, medical applications, and more.

The aim of the jubilee 10th National Norwegian NMR Meeting is to gather together Norwegian researchers working in this field to discuss recent achievements related to the different applications of NMR methodology obtained at the national level since the last national meeting in 2006. This year, the conference takes place at the Quality Hotel in Oppdal, a place that is known for its great winter sport entertainment activity. Therefore, we hope that the conference participants will enjoy both high quality scientific program and sport social program.

As can be seen from the scientific program and submitted abstracts for talks and posters, a broad range of application areas in NMR will be covered. We would like to thank all the contributors that made it possible for us to put together a program of such high diversity and quality. This year, we are also happy to include in our program three invited lectures that will be delivered by leading international NMR scientists.

We wish you all a great meeting,

The organizing committee:

Alexander Dikiy

John Georg Seland

10th National Norwegian NMR Meeting, Oppdal, Norway, 16-18 January 2008

Wednesday		
09.00-13.00	**Registration**	
13.00-14.00	**Lunch**	
14.00-14.15	**Welcome**	
	Session 1: Biomedical applications and NMR in food	**Chairman: O. Haraldseth**
14.15-15.00	**Ross Mair**; Use of hyperpolarized noble gas MRI to study human lung function	
15.00-15.30	**Øystein Risa;** Acute and chronic hydocephalus monitored by *in vivo* ^{1}H NMR Spectroscopy and MR Imaging	
15.30-16.00	**Coffee Break**	
16.00-16.30	**Ingrid S Gribbestad**; Diagnosis of Cancer using High Resolution MAS MR Spectroscopy	
16.30-17.00	**Beathe Sitter**; Absolute quantification of breast cancer metabolites using ERETIC in HR MAS MR spectroscopy	
17.00-17.30	**Emil Veliyulin**; Quantitative ^{23}Na MRI of muscle foods	
17.30-18.00	**Marte Thuen**; Manganese-enhanced MRI of the optic nerve	
18.00-19.00	**Poster Session**	
19.30-	**Dinner**	
Thursday		
09.00-13.00	**Skiing**	
13.00-14.00	**Lunch**	
	Session 2: Solid state NMR and material science	**Chairman: J. G. Seland**
14.00-14.45	**Janez Stepišnik**; Molecular and granular translational dynamics measured by a novel NMR technique	
14.45-15.15	**Kate E Washburn**; Novel Nuclear Magnetic Resonance Techniques for Materials Characterization	
15.15-15.45	**Coffee Break**	
15.45-16.15	**Andreas N Berntsen**; Quantitative Investigation of Formation Damage in Sandstones Using Low-Field NMR	
16.15-16.45	**Magnus Jensen**; Anticancer Cisplatin Interacting with Bilayer of Total Lipid Extract from Pig Brain: A ^{13}C, ^{31}P and ^{15}N Solid-State NMR Study	
16.45-17.15	**Eddy W Hansen**; Spin Diffusion – Principles and Application	
17.15-17.45	**Signe Steinkopf**; Water and Heptanol Interaction with Non-porous Silica Surface: A ^{1}H Solid-State NMR Study	
18.00-19.00	**Election of members to the NMR Spectroscopy National Committee**	
19.30-	**Dinner**	
Friday		
	Session 3: High-resolution liquid NMR	**Chairman: A. Dikiy**
09.00-09.45	**Göran Karlsson;** title to be announced later	
09.45-10.15	**Einar Sletten**; NMR kinetic studies using isotope labeled reagents	
10.15-10.30	**Coffe Break**	
10.30-11.00	**Finn Aachmann**; Solution Structure of Selenoprotein W and NMR analysis of its interaction with 14-3-3 proteins	
11.00-11.30	**Lars Skjeldal**; Membrane binding of cyclic polypeptides	
11.30-12.00	**Trond R Størseth**; Differences in metabolic and transcript composition between wild type and genetically modified *Arabidopsis thaliana* studied by ^{1}H NMR metabolomics and microarray	
12.00-12.30	**Closing**	
12.30-13.30	**Lunch**	

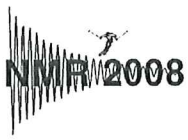

ABSTRACTS FOR ORAL CONTRIBUTIONS

Use of hyperpolarized noble gas MRI to study human lung function

R. W. Mair

[1] Harvard-Smithsonian Center for Astrophysics, Cambridge, MA, USA.

In recent years, MRI of inhaled, hyperpolarized ^{3}He gas [1,2] has emerged as a powerful method for studying lung structure and function [3,4]. ^{3}He hyperpolarized to 30–60% can be created by one of two laser-based optical pumping processes [1,2] prior to the MRI procedure. Such high spin polarization gives ^{3}He gas a magnetization similar to that of water in ~ 10 T fields, despite the drastically lower spin density of the gas. This permits high-resolution gas space imaging to be performed with SNR and image quality similar to that of conventional ^{1}H MRI [3,4]. This technique has been used to make quantitative maps of human ventilation [5], obtain regional acinar structural information via measurements of the ^{3}He Apparent Diffusion Coefficient (ADC) [6], and to monitor the regional O_2 concentration (p_AO_2) via the ^{3}He spin-relaxation rate [7,8]. These techniques have applications to basic pulmonary physiology [9] as well as lung diseases such as asthma and emphysema [9,10]. A brief overview of work in this field will be presented.

A key measure of the effectiveness of pulmonary ventilation and perfusion is the alveolar partial pressure of oxygen, p_AO_2. MRI using hyperpolarized ^{3}He has, in recent times, provided the first regionally-selective measure of p_AO_2 [7,8], which has been correlated with the traditional ventilation-to-perfusion ratio, *V/Q* [8]. Gravity induces vertical gradients in transpulmonary and pulmonary vascular pressures leading to regional heterogeneity of pulmonary ventilation and perfusion, which in turn induces a vertical p_AO_2 gradient [11,12]. Non-invasively observing the effect of gravity or posture on lung physiology has been a challenge because clinical scanners restrict subjects to a horizontal position.

Some initial studies with hyperpolarized ^{3}He have shown that posture changes, even while horizontal, affect the lung structure modestly in a way that can nonetheless be clearly probed by ^{3}He MRI [13]. To enable complete posture-dependent lung imaging, we have developed an open-access MRI system based on a simple electromagnet design that operates at a field strength ~ 200 times lower than a traditional clinical MRI scanner [14,15]. To perform MRI at such a field strength, we exploit the practicality of hyperpolarized ^{3}He MRI at magnetic fields < 10 mT [16-19]. As the ^{3}He gas is spin-polarized by the laser-based, optical pumping process, the large magnetic field associated with traditional MRI scanners is no longer required.

Our open-access human MRI system was optimized to operate at B_0 = 6.5 mT (65 G), allowing ^{3}He MRI at 210 kHz [14-15]. Polarized ^{3}He gas (~ 500 cm^3) was transferred from a home-built spin-exchange polarizer to a plastic sampling bag. This bag was either used a phantom, or as the source of ^{3}He gas for inhalation by human subjects. 2D and 3D gradient-recalled-echo images have been acquired to show ventilation patterns, changes in lung shape as a function of posture, and variation of regional p_AO_2 with posture.

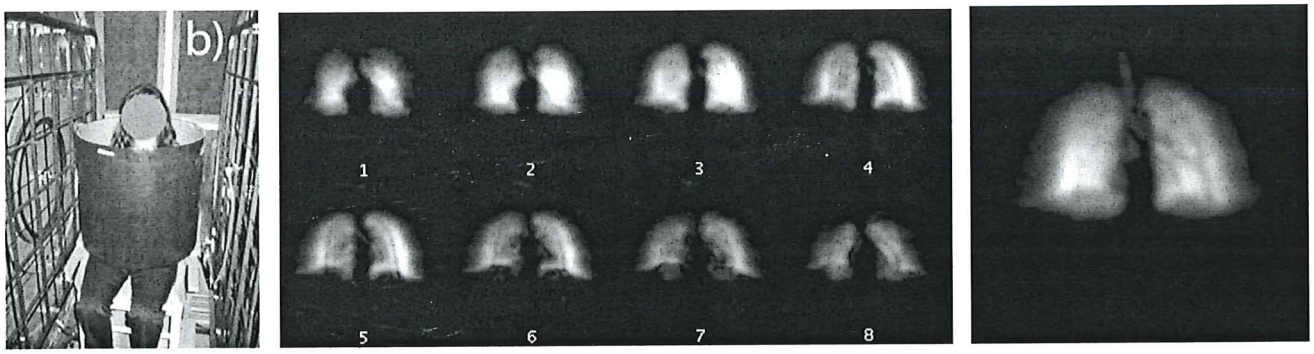

Figure: Left: Subject sitting vertically in the open-access human MRI system. Center: ~ 1.5 cm thick horizontal slices from a 3D image dataset obtained while the subject was supine. Right: 2D projection image acquired while the subject was vertical.

References

1. T.G. Walker, W. Happer, *Rev. Mod. Phys.* **69**, 629-642 (1997).
2. P.J. Nacher, M. Leduc, *J. Physique*, **46**, 2057-2073 (1985).
3. J. Leawoods, et al, *Concepts Magn. Reson.* **13**, 277-293 (2001).
4. H.E. Moller, et al, *Magn. Reson. Med.* **47**, 1029-1051 (2002).
5. J.M. Wild, et al, *Magn. Reson. Med.* **49**, 991-997 (2003).
6. M. Salerno, et al, *Radiology*, **222**, 252-260 (2002).
7. A.J. Deninger, et al, *NMR Biomed.* **13**, 194-201 (2000).
8. R.R. Rizi, et al, *Magn. Reson. Med.* **52**, 65–72 (2004).
9. G.H. Mills, et al, *British Journal of Anaesthesia.* **91**, 16-30 (2003).
10. S. Samee, et al, *J. Allergy Clin. Immunol.* **111**, 1205-1211 (2003).
11. G. Musch et. al., *J. Appl. Physiol.*, **93**, 1841-1851 (2002).
12. J. West, *Respiratory Physiology-The Essentials* (1995).
13. S. Fichele et al, *J. Magn. Reson. Imaging* **20**, 331-335 (2004).
14. L.L. Tsai, R.W. Mair, et al, *Acad. Radiol.* in press (2008).
15. L.L. Tsai, R.W. Mair, et al, *J. Magn. Reson.* submitted (2007).
16. C.H. Tseng, et al, *Phys. Rev. Lett.* **81**, 3785-3788 (1998).
17. G.P. Wong, et al, *J. Magn. Reson.* **141**, 217-227 (1999).
18. R.W. Mair, et al. *Magn. Reson. Med.* **53**, 745–749 (2005).
19. I.C. Ruset, R.W. Mair, et al. *Concepts Magn. Reson. – Magn. Reson. Eng.* **29B**, 210–221 (2006).

Acute and chronic hydocephalus monitored by *in vivo* ^{1}H MR Spectroscopy and MR Imaging

Daniel Kondziella [1,2], Øystein Risa [1], Elvar M. Eyjolfsson [1], Ursula Sonnewald [1]

[1] Department of Neuroscience, Norwegian University of Science and Technology, Trondheim, Norway

[2] Department of Neurology, Sahlgrenska University Hospital, Göteborg, Sweden

Hydrocephalus is one of the few reversible causes of dementia and recent epidemiological studies have shown that normal pressure hydrocephalus (NPH) has a far higher prevalence than earlier estimated. Since dementia is an increasing socioeconomic problem, NPH and other forms of chronic hydrocephalus have become a hot topic in clinical neurology. This coincides with a recent paradigm shift in hydrocephalus research: In contrast to earlier doctrines, chronic hydrocephalus is now considered as much a disorder of cellular metabolism as of cerebrospinal fluid (CSF) dynamics. The kaolin model allows the study of hydrocephalus turning from the acute into the chronic state and as such, might help in the establishment of non-invasive diagnostic tools, which would have great clinical impact. Thus, 27 rats were made hydrocephalic by injection of 0.1 ml kaolin into the cisterna magna. Using a 7-tesla magnet, *in vivo* ^{1}H Magnetic Resonance Spectroscopy (MRS) and Magnetic Resonance Imaging (MRI) were performed longitudinally two, four and six weeks later. In hydrocephalic animals, a clear lactate peak was detected on spectra from CSF and T_2-weighted images showed increase of free water in the hippocampus, but not thalamus. Hippocampal edema probably contributes to the development of dementia in hydrocephalic patients. It can be concluded that longitudinally MRS and MRI enable non-invasive monitoring of transformation from acute into chronic kaolin-induced hydrocephalus.

Diagnosis of Cancer using High Resolution MAS MR Spectroscopy

Ingrid S. Gribbestad, Ph.D., Tone F. Bathen, Ph.D. and Beathe Sitter, Ph.D.
Department of Circulation and Medical Imaging, Norwegian University of Science and Technology, Trondheim, Norway

Introduction

The MR spectroscopy (MRS) method gives a comprehensive window into tissue biochemistry and interrogates cancer tissue for diagnostic and prognostic markers. High resolution magic angle spinning (HR MAS) MRS is a high-throughput technology with increased spectral resolution compared to conventional MR spectroscopy. Its non-destructive nature allows specimens to be evaluated by histopathology after spectral analysis. Findings from brain (1-3), cervical (4,5), breast (6), and prostate cancer (7,8) have proven HR MAS as a promising tool in cancer diagnosis and treatment monitoring. The objective of this presentation will be to describe the HR MAS MRS techniques and clinical use related to different cancer types.

High-resolution magic angle spinning (HR MAS) MR spectroscopy

Lack of molecular mobility in tissue leads to anisotropic interactions and gives broad lines in ex vivo spectra. The line broadening can be reduced by spinning the sample rapidly about an axis inclined 54.7° to the direction of the static magnetic field. The anisotropic interactions are dependent on $(3\cos^2\theta-1)$ and will be cancelled by this angle. Suppression of signals with short T_2 values can be obtained using a spin-echo sequence with long echo times. Cancer tissue samples comprise a vast amount of MR detectable compounds and the resulting spectra can be very complex (Figure 1).

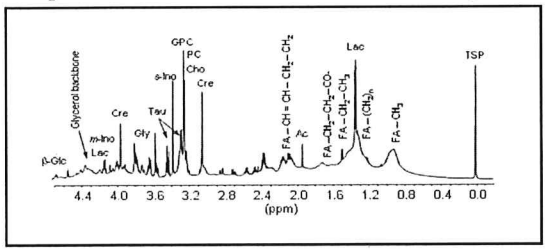

Figure 1. Standard HR MAS pulse-acquired spectrum of cervical cancer biopsy with a tumor cell fraction of 85%. Spectral assignments are abbreviated: β-Glc, β-glucose; Lac, lactate; m-Ino, myo-inositol; Cre, creatine; Gly, glycine; Tau, taurine; s-Ino, scyllo-inositol; GPC, glycerophosphocholine; PC, phosphocholine; Cho, choline; FA, fatty acids (the position of hydrogens in fatty acids giving rise to the different peaks is marked in bold after the notation FA); Ac, acetate; and TSP, trimethylsilyl propionic acid.

Metabolic ratios or quantification of metabolites are used to extract information from HR MAS MR spectra. However, quantification of HR MAS signals from biological tissue is a challenge due to visibility of internal standards. Spin-echo experiments will cause a T_2 dependence of spectral signals that must be corrected for. Recently, the ERETIC method (9) which generate an electronically synthesized reference signal has been implemented in HR MAS analyses (10). Multivariate data analysis is commonly used for exploration, classification and prediction since several studies have shown that multiple resonances influence the spectral patterns (6, 11-13).

Current clinical research

Ex vivo HR MAS MRS provide detailed descriptions of the metabolic pattern in tissue specimens from different cancers (1-6, 13-15). Studies of brain tissue have shown that metabolites ratios correlate to density of specific cell types (16) and to the fraction of cancerous and necrotic areas (17). In HR MAS studies of prostate tissue, metabolite concentration has been found to correlate to tissue composition (15) and to discriminate malignant prostate from healthy glandular tissue (15, 18). Breast carcinoma tissue can be distinguished from non-involved breast tissue (6,14) and tumor grade and lymph node status can be predicted (13). The HR MAS technique is now also being explored as a tool for assessing treatment effects. Studies involving chemotherapeutic agents and radiation therapy have been presented using animal models (18,19) and human tissue samples (20, 21). In summary, HR MAS MRS is proving to give valuable clinical information which is now being tested in larger clinical studies.

References

1. Cheng LL et al. Cancer Res (1998) 58: 1825-1832; 2. Martinez-Bisbal MC et al. NMR Biomed. (2004) 17: 191-205; 3. Tzika AA et al. J. Neurosurg. (2002) 96: 1023-1031; 4. Mahon MM et al. NMR Biomed. (2004) 17: 144-153; 5. Sitter B et al. MAGMA. (2004) 16: 174-181; 6. Sitter B et al. NMR Biomed. (2006), 19 , 30-40; 7. Swanson MG et al. Magn Reson Med (2003) 50: 944-954; 8.Burns MA et al Technol Cancer Res Treat. (2004) 3(6):591-8; 9. Silvestre V et al. Anal.Chem. (2001) 73: 1862-1868; 10. Sitter B et al. ISMRM Cancer workshop 2006; 11. el Deredy W et al. NMR Biomed (1997) 10: 99-12; 12. Lindon JC et al. Prog Nucl Magn Res Spec (2001) 39: 1-40; 13. Bathen TF et al. Breast Cancer Res Treat. (2007) 104(2):181-9; 14. Sitter B et al. NMR Biomed (2002) 15: 327-337; 15. Moka D et al. Journal of Pharmaceutical & Biomedical Analysis (1998) 17: 125-132; 16. Cheng LL et al. Magn Reson Imaging (2002) 20: 527-533; 17. Tzika AA et al. J Neurosurgery (2002) 96: 1023-1031; 18. Valonen PK et al. NMR Biomed. (2005) 18: 252-259; 19. Morvan D et al. Cancer Res. (2002) 62: 1890-1897; 20. Chen JH et al. Magn Reson Med (2002) 48: 602-610; 21. Lyng H et al. BMC Cancer (2007) Jan 17;7:11.

(Dette abstraktet er delvis publisert på International Society of Magnetic Resonance in Medicine, Annual Meeting 2007)

Absolute quantification of breast cancer metabolites using ERETIC in HR MAS MR spectroscopy

B. Sitter[1], T. F. Bathen[2], T. E. Singstad[3], J. Halgunset[4], S. Lundgren[5,6], and I. S. Gribbestad[1]

[1]Department of Circulation and Medical Imaging, NTNU, Trondheim, Norway, [2]Department of Circulation and Medical Imaging, NTNU, Trondheim, [3]Department of Radiology, St. Olavs University Hospital, Trondheim, Norway, [4]Department of Laboratory Medicine, Children's and Women's Health, NTNU, Trondheim, Norway, [5]Cancer Clinic, St. Olavs University Hospital, Trondheim, Norway, [6]Department of Cancer Research and Molecular Medicine, NTNU, Trondheim, Norway

Background

High-resolution magic angle spinning (HR MAS) MR spectra of cancerous tissue combined with multivariate analysis is a promising tool in cancer diagnostics (Bathen 2006). To truly obtain detailed knowledge about biochemical processes in cancerous tissue, there is a need for improved methods for absolute quantification avoiding internal standards that can associate to the tissue (Kriat 1992). ERETIC (Electronic REference To access In vivo Concentrations) appears to be a very promising method (Barantin 1997), by using a synthetic rf signal first calibrated to a reference compound. The ERETIC method has been evaluated in high-resolution MR spectroscopy (Akoka 1999). The purpose of this study was to implement absolute quantification of HR MAS spectra using the ERETIC method and correlate this to the histopathologically determined tumor fraction.

Experimental

Breast cancer samples (n=10, invasive ductal carcinomas, grade II (n=4) and III (n=6)) were cut to fit a zirconium rotor (50 µL) and added 40 µL phosphate buffered saline (PBS) containing TSP (10 mM). Excess fluid was removed and weights of buffer and sample were accounted for by repeated weighing of the rotor in the assembling procedure. Five different solutions of creatine (10, 5, 2.5, 1 and 0.25 mM) in PBS with TSP (10 mM) were prepared for quantification and calibration of the ERETIC signal. HR MAS experiments were performed on a Bruker AVANCE DRX600 spectrometer (spin rate 5 kHz, 4 °C). A pulse-acquired experiment including the ERETIC sequence (ereticpr.drx; Bruker) was performed for all solutions and samples. The ERETIC signal was obtained using a 40 dB attenuator, a pulse level of 35 dB and positioned at -1.0 ppm. Signals were collected over a sweep width of 16.7 ppm, and128 FIDs were collected into 64K points during 3.28 seconds. Peak areas were calculated by curve fitting (PeakFit, Jandel), of creatine, TSP and ERETIC signals in spectra of solutions, and in addition glycine, taurine, glycerophosphocholine (GPC), phosphocholine (PC) and choline signals in spectra from tissue samples. The ERETIC signal was calculated from the CH_3-signal in spectra (n=17) of the 10 mM creatine solution to correspond to 4.22×10^{-7} moles. This value was calibrated using five spectra from each of the five different solutions of creatine. After HR MAS analysis, tissue specimens were fixed in 10% formalin and embedded in paraffin. The relative areas of normal and neoplastic epithelial elements, fat and fibrous connective tissues were scored visually by a pathologist. Metabolite concentrations were compared to tumor fraction by Pearson correlation analysis (SPSS).

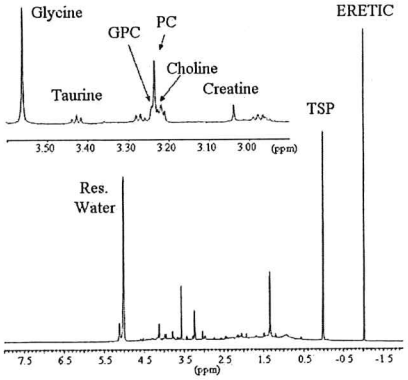

Figure 1 Spectral region 8.0 - -2.0 ppm of HR MAS spectrum of breast cancer sample obtained by the ERETIC method. Region of selected metabolites for quantification is expanded. Abbreviations: GPC; glycerophosphocholine and PC; phosphocholine.

Results

Calibration of the ERETIC signal showed that creatine concentrations were calculated by an accuracy of at least 5.4% using the ERETIC signal compared to 3.8% using the internal reference TSP. A HR MAS spectrum of a breast cancer sample recorded using the ERETIC sequence is shown in Figure 1. Histopathological evaluation showed that tumor content in the breast cancer specimens varied from 0 to 70%. The two methods for finding metabolic concentrations gave similar results for most breast tissue samples, mean values are shown in Table 1. Significant correlation to tumor fraction was found for choline and creatine. The tumor content is linearly correlated with a Pearson correlation factor of 0.66 (p = 0.37) to the concentration of choline, and 0.79 (p=0.007) to the concentration of creatine. When the outlier in the plot of glycine (Figure 2) was excluded we found a Pearson correlation factor of 0.97 (p< 0.001) between tumor fraction and tissue concentration of glycine.

Table 1 Mean tissue metabolic concentrations (µmol per gram tissue) of metabolites estimated from HR MAS spectra of intact breast cancer specimens using the ERETIC signal (upper values) and TSP as an internal reference (lower values). Standard deviations are given in brackets.

	Glycine	Taurine	GPC	PC	Choline	Creatine
ERETIC	1.27 (±1.11)	1.47 (±0.72)	0.33 (±0.22)	0.69 (±0.74)	0.33 (±0.17)	0.55 (±0.38)
TSP	1.65 (±2.04)	1.76 (±1.29)	0.41 (±0.40)	0.88 (±1.10)	0.40 (±0.29)	0.64 (±0.47)

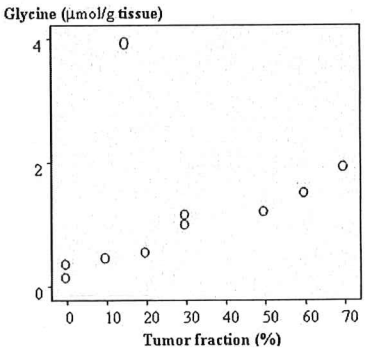

Figure 2 Breast tissue metabolic concentrations of glycine calculated from the ERETIC signal plotted against tumor fractions.

Discussion

Tissue metabolite concentrations were found to be lower in one sample and higher in three when using TSP as a reference compared to the ERETIC signal. We find it likely that TSP is the more unreliable reference, as the concentration of TSP is depending on accurate measures of fluid loss in rotor assembly and TSP possibly binds to tissue compounds. The correlation found between metabolite concentrations and tissue composition shows that measured concentration of metabolites such as choline and glycine depend on the amount of tumor tissue in the sample. Therefore, for absolute quantification it is important to correct for the tumor fraction. In conclusion, the ERETIC method can be used to quantify metabolites in tissue samples by an accuracy of at least 5%.

References

Akoka, S et al. *Analytical Chemistry* **71** (1999)
Barantin, L et al. *Magn Reson.Med.* **38** (1997)
Bathen, TF et al. *Breast Cancer Res.Treat.* (2006)
Kriat, M et al. *NMR in Biomedicine* **5** (1992)

☒ preferred ORAL presentation ☐ POSTER presentation

Quantitative ^{23}Na MRI of muscle foods

E. Veliyulin[1], B. Egelandsdal[2], F. Marica[3] and B.J. Balcom[3]

[1] SINTEF Fisheries and Aquaculture, N-7465 Trondheim, Norway
[2] Institute of Food Research, University of Agriculture, N-1432, Ås, Norway
[3] MRI Centre, Department of Physics, University of New Brunswick, Fredericton, NB, Canada E3B 5A3

Abstract:
Quantitative sodium analysis in muscle foods by ^{23}Na MRI is traditionally considered problematic because of the well-known partial MRI sodium "invisibility" phenomenon reported earlier [1,2]. Partial ^{23}Na "invisibility" is often referred to as an inherent drawback of the MRI technique, impairing the quantitative sodium analysis.
Several model samples were designed to simulate muscle foods with a broad variation in the protein, fat, moisture and salt content. Spin-echo MRI technique and a recently developed SPRITE MRI approach [3,4] were applied for quantitative sodium imaging. Typical sodium images generated by these two methods from the same sample are shown in Fig. 1. Substantial underestimation of the salt content by the spin-echo technique and good correspondence between the SPRITE MRI sodium content and that determined by the reference chemical method were found. Thus the applicability of SPRITE MRI approach for accurate sodium quantification was demonstrated. ^{23}Na free induction decay and CPMG relaxation experiments were performed on the same sample set as well, additionally confirming that the sodium "invisibility" is rather a methodological problem that can easily be circumvented by using SPRITE MRI technique.

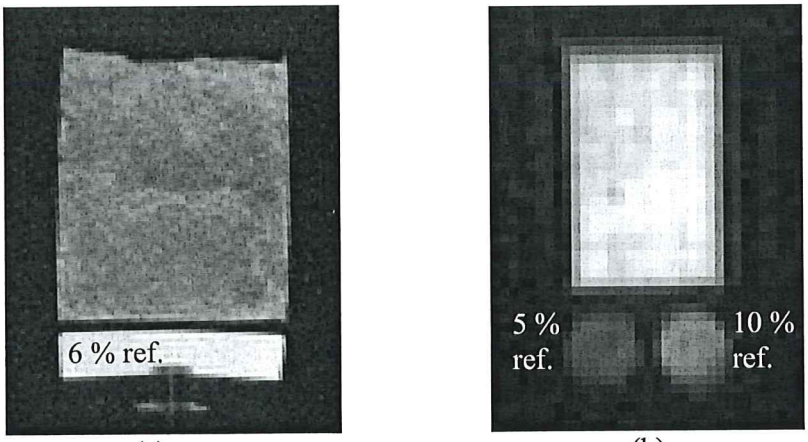

(a) (b)

Fig.1: (a) Spin-echo MRI and (b) SPRITE MRI image of the same sample. Salt content determined chemically was 15.8 %.

1. Springer, C.S., Ann. Rev. Biophys. Biophys. Chem., **16** (1987) 375-399
2. Shapiro, E.M., Borthakur, A., Dandora, R., Kriss, A., Leigh, J.S. and Reddy, R., J. Magn. Res., **142** (2000) 24-31
3. B.J. Balcom, R.P. MacGregor, S.D. Beyea, D.P. Green, R.L. Armstrong and T.W. Bremner, *J. Magn. Reson. Series A* **123** (1996) 131-134
4. M. Halse, D.J. Goodyear, B. MacMillan, P. Szomolanyi, D. Matheson and B.J. Balcom, *J. Magn. Reson.* **165** (2003) 219-229

Manganese-enhanced MRI (MEMRI) of the optic nerve

Marte Thuen[1], Øystein Olsen[2], Martin Berry[3], Axel Sandvig[4], Pål Erik Goa[5], Olav Haraldseth[1, 5], Christian Brekken[1]

[1]Department of Circulation and Medical Imaging, NTNU, Trondheim, Norway
[2]Department of Radiography, Sør-Trøndelag University College, Trondheim, Norway
[3]Molecular Neuroscience, University of Birmingham, Birmingham, United Kingdom
[4]Laboratory of Regenerative Neurobiology, NTNU, Trondheim, Norway
[5]Department of Medical Technology, St. Olavs Hospital, Trondheim, Norway

Introduction: Manganese-enhanced MRI of the optic nerve (ON) is based on the two main principles that

1) Manganese is paramagnetic and reduces T1, which gives contrast enhancement in MR images.
2) Manganese is a calcium analogue that can be taken up axons and transported along neural pathways.

This makes manganese a unique contrast agent well suited for MRI of neural pathways in the animal brain.

The presentation will include the main findings obtained in our laboratory during the past few years.

Materials and methods: MRI was performed at 2.35T or 7T using Bruker Biospec small animal scanners 24-48h after injection of $MnCl_2$ into the vitreous body. Laboratory animals such as rats, mice, frogs and fish with normal or injured optic nerves were used, and a sophisticated post-processing tool involving semi-automatic segmentation of the optic nerve was developed.

Results and discussion: The entire visual pathway from the retina to the superior colliculus was enhanced 24h after injection of 200nmol $MnCl_2$ and MEMRI detected optic nerve crush (ONC). $MnCl_2$ is non toxic to retinal ganglion cells (RGC) after the doses needed to obtain a sufficient Mn^{2+}-contrast in MRI (150-300nmol), but is toxic after high doses ($\geq$1500nmol), causing major RGC death and lack of Mn^{2+}-enhancement throughout the visual pathway. This demonstrates that viable axons are needed for the active transport Mn^{2+}. 22d after ONC and implantation of a peripheral nerve graft (PNG), increased contrast was seen distal to the crush site, indicating that MEMRI can be used to detect regeneration in the adult rat CNS.

Molecular and granular translational dynamics measured by a novel NMR technique

Janez Stepišnik
Faculty of Mathematics and Physics, University of Ljubljana, Slovenia

Novel NMR spin echo technique with a unique feature to scan the spectrum of spin displacement in the frequency range between a few Hz and to above 10 kHz is presented. The method enables wide range of application: to analyze the low frequency range of anomalous molecular diffusion of ordinary liquids, to study the self-diffusion of fluids confined in porous or gelatinous structure, to measure directly the velocity auto-correlations of grains in a fluidized granular systems etc. Recent results give new insight into dynamics of those systems that also enables characterization of their structure.

Novel Nuclear Magnetic Resonance Techniques for Materials Characterisation

Kate E. Washburn[a], Paul T. Callaghan[a], Christoph H. Arns[b]

a) School for Chemical and Physical Sciences, MacDiarmid Institute for Advanced Materials and Nanotechnology, Victoria University of Wellington, New Zealand

b) Department of Applied Maths, Research School of Physical Sciences and Engineering, Australian National University, Australia

Porous media are ubiquitous materials important to a wide range of disciplines such as oil recovery, chemical engineering, biology and materials science. However, the behaviour of fluids within a porous medium is often poorly understood. Nuclear magnetic resonance is a common technique used in porous media research. While most of our experimental work has focused on porous media, our techniques have shown potential for use in soft condensed matter and complex materials.

The transverse relaxation time is known to be correlated with pore size; in general the smaller the pore, the shorter the relaxation time. We use this behaviour to tag the location of fluid molecules at two points in time that are separated by a mixing period. A change in the T_2 value between the two encode intervals indicates a change in environment and suggests the molecule has diffused to a new pore. By performing experiments for a range of mixing time, we can observe how the number of molecules that remain in their original environment and those that shift environment change as a function of time.

A limit of the T_2-relaxation exchange experiment is that it cannot differentiate between the signal that comes from spins in their original pore and the signal from molecules that have diffused to a pore of a similar size. We perform a diffusion encode over the mixing time to better understand the movement of the fluid molecules during this period, combining two inverse Laplace dimensions with a Fourier dimension. The data is Fourier transformed along the diffusion axis to obtain the average propagator. Planes of T_2-T_2 exchange experiments are then extracted from along the propagator and inverted using the 2D inverse Laplace transform. The peak intensities are integrated and plotted as a function of mixing time and displacement. Using a non-linear least squares regression to fit the experimental results to theory, we can estimate important physical quantities such as pore size, inter-pore spacing, pore characteristic time, and tortuosity.

Quantitative Investigation of Formation Damage in Sandstones Using Low-Field NMR

Andreas N. Berntsen, NTNU

When drilling for hydrocarbons, drilling mud will be filtrated by the porous formations due to an overpressure in the well. A low-permeability filter cake will form on the rock surface, and impair further outflow. Mud filtrate in the formation may not be completely removed upon onset of reservoir oil production. This can cause a reduction in porosity and/or hydraulic permeability, termed formation damage. Knowledge of the formation damage potential of drilling muds is an important aspect of petroleum engineering. For production to commence in an open-hole completion, the oil must flow through the potentially formation damaged zone, and through the filter cake. The filter cake may yield in two ways; either it detatches in large slabs, or it deforms locally, creating small "pinholes". In many cases pinholing may be preferential, to prevent pieces of cake clogging completion equipment. It is believed that the failure mode is in part determined by the two-phase flow behind the cake.

In this study, water-based muds are filtrated through sandstone cores brought to irreducible water saturation by flooding them with brine, then with lamp oil, so as to mimic reservoir conditions. The cores are then backflooded with oil to simulate oil production. 2 MHz ^{1}H NMR is employed to study the T_2 distribution of the cores at each stage. The results show that the initial distributions are not restored after backflooding. The changes are interpreted as remaining formation damage, probably due to particle clogging and changes in oil saturation. It is thought that a probable mechanism responsible for this remaining formation damage is viscous fingering of produced oil into the mud filtrate in place. The prediction of filter cake failure mode by NMR relaxometry is discussed in light of this finding.

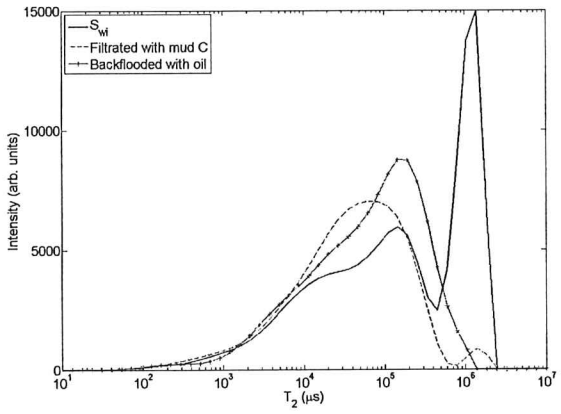

Figure 1: *T_2 distributions of a sandstone core at three different stages: "virgin" conditions, after filtrating with WBM, and then after backflooding with oil. It is clear that the initial saturation state is not restored upon backflood.*

Anticancer Cisplatin Interacting with Bilayer of Total Lipid Extract from Pig Brain: A ^{13}C, ^{31}P and ^{15}N Solid-State NMR Study

Magnus Jensen and Willy Nerdal

Department of Chemistry, University of Bergen, Allegaten 41,

N-5007 Bergen, Norway.

Abstract

^{13}C MAS NMR spectra of total lipid extract from pig brain with and without 10 mol% cisplatin show that the phosphatidylserine (PS) carboxyl resonance (at 171.5 ppm in spectrum of pure lipid) and the serine head group β-carbon resonance both disappear in presence of cisplatin and that a new resonance of similar intensity appears at 185 ppm. Thus, indicating cisplatin interaction with the phosphatidylserine head group.

Static ^{31}P NMR spectra of lipid extract with and without 10 mol% cisplatin show that the phosphorous containing lipids to a large extent reside in a bilayer environment in pure lipid extract, and that the presence of cisplatin introduces new lipid phases.

^{15}N MAS spectra of total lipid extract from pig brain with 10 mol% show a large resonance at -80 ppm, the ^{15}N resonance of ($[Pt(NH_3)_2Cl(OH_2)]^+$), and smaller resonances around -100 ppm from lipid bound cisplatin.

Spin Diffusion - Principles and Application

Eddy W. Hansen, Department of Chemistry, UiO, P.O.Box 1033, Blindern
E-mail: eddywh@kjemi.uio.no

A brief outline of the principles of "spin-diffusion" (SD) is presented, and its relevance in polymer chemistry is exemplified for semi-crystalline polyethylene.

Water and Heptanol Interaction with Non-porous Silica Surface: A ^{1}H Solid-State NMR Study

Signe Steinkopf[§] and Willy Nerdal *

[§]Bergen University College

Department of Chemistry,

University of Bergen, Norway.

Abstract

Colloidial, nonporous and uniform silca particles with a diameter of 40 nm were used in this study as a model rock carrying water and hydrocarbon.

Static ^{1}H-NMR spectra displays immobilization of fluid by the presence of very broad water/hydrocarbon resonances. Detailed information about the interaction at the silica surface is obtained by ^{1}H-MAS NMR where the spin-lattice (T_1) relaxation behavior of water and heptanol is monitored as a function of temperature. Water demonstrates higher immobilization than heptanol in presence of the silica surface. Both H_2O and heptanol ^{1}H T_1 measurements demonstrate temperature dependence that indicate molecular mobilities in the extreme narrowing motional regime in the higher sample temperatures studied. In the lower temperature range studied, both H_2O and heptanol show a ^{1}H T_1 relaxation dependence on temperature that indicates simultaneous presence of several molecular correlation times.

Title to be announced

Göran Karlsson

Swedish NMR Centre, Göteborg University, Gothenburg, Sweden

NMR kinetic studies using isotope labelled reagents.

Einar Sletten and Nils Åge Frøystein,
Department of Chemistry, University of Bergen

The rapid development of NMR spectroscopic methods and instrumentation has enabled us to investigate relative complicated reaction path ways in coordination chemistry. In order to follow chemical reactions by NMR we need to record spectra at sufficient speed and S/N to determine quantitative concentrations of reaction intermediates. Firstly, the advent of cryo-probes has greatly improved S/N at short time interval. Secondly, the inverse detection methods have proven to be the method of choice, either HMQC (Heteronuclear Multiple Quantum Coherence) or HSQC (S= single) for these type of measurements[1]

The procedure involves the following steps: i) assigning the cross-peaks in a set of time-dependent inverse spectra; ii) integration of cross-peaks; iii) suggest a reaction path way; iv) constructs a set of differential rate equations; v) carry out a non-linear optimisation least-squares calculation to obtain the best fit to the spectral intensities vs time data.

Results will be presented for the reaction between ^{15}N labelled cytotoxic platinum ammine complexes and a DNA mononucleotide [2]

Reference.
1. G. Bodenhausen and D.J. Ruben. *Chem. Phys. Lett.* 1980, **69**, 185.
2. J.Vinje, F.P. Intini, G. Natile, E. Sletten. *Chem.Eur. J.* 2004, **10**, 3569

Solution Structure of Selenoprotein W and NMR analysis of its interaction with 14-3-3 proteins

Finn L. Aachmann[a], Dmitri E. Fomenko[b], Alice Soragni[a], Vadim N. Gladyshev[b] and Alexander Dikiy[a]

[a] Department of Biotechnology, Norwegian University of Science and Technology, N-7491 Trondheim, Norway and [b] Department of Biochemistry, University of Nebraska, Lincoln, Nebraska 68588, USA.

Selenium is a trace element with significant biomedical potential. It is essential in mammals due to occurrence in several proteins in the form of selenocysteine (Sec). One of the most abundant mammalian Sec-containing proteins is selenoprotein W (SelW). This protein of unknown function has a broad expression pattern and contains a candidate CxxU (U is Sec) redox motif. Here, we report solution structure of Sec13Cys variant of mouse SelW determined through high resolution NMR spectroscopy. The protein has a thioredoxin-like fold with the CxxU motif located in an exposed loop similarly to the redox-active site in thioredoxin. Protein dynamics studies revealed rigidity of the protein backbone and mobility of two external loops and suggested a role of these loops in interaction with SelW partners. Molecular modeling of structures of other members of the Rdx family based on the SelW structure identified new conserved features in these proteins, including an aromatic cluster and interacting loops. Our previous study suggested an interaction between SelW and 14-3-3 proteins. In the present work, with the aid of NMR spectroscopy, we demonstrated specificity of this interaction and identified mobile loops in SelW as interacting surfaces. This finding suggests that 14-3-3 is a redox regulated protein.

Membrane binding of cyclic polypeptides

Lars Skjeldal

Department of Chemistry, Biotechnology and Food Science
Norwegian University of Life Sciences

Differences in metabolic and transcript composition between wild type and genetically modified *Arabidopsis thaliana* studied by ^{1}H-NMR metabolomics and microarray.

Diem Hong Tran[a], Tommy Jørstad[a], Per Winge[a], Trond R. Størseth[b] and Atle Bones[a]

[a] Department of Biology, Norwegian University of Science and Technology, 7491 Trondheim, Norway
[b] Department of Marine Resources Technology, SINTEF Fisheries and Aquaculture, 7465 Trondheim, Norway

Arabidopsis thaliana is a model plant for studying plant sciences, including plant defence and development. Glucosinolates (GS) are a class of secondary metabolites with important roles in plant defence and may also influence plant growth and development. In addition, they are important for humane life. Some degradation products of GS are flavour compounds and some exhibit anticarcinogenic properties. To understand the functions of GS in plants, an integrated approach has been undertaken to study a mutant, *cyp83B1*, impaired in the GS biosynthesis pathway. A comprehensive study, including micro array analysis with full-genome chips and metabolite analysis including ^{1}H-NMR and LC-MS techniques could provide in dept-understanding of the functions of GS and CYP83B1 in particular. Here the focus is on ^{1}H-NMR.

For ^{1}H-NMR analysis 50% MeOD in KH_4PO_4 buffered D_2O (pH=6) was used to extract lyophilized plant material. Each plant was divided into root and leaf (n=4 for each group). TSP was used as an internal reference. The samples were analyzed at 298 K on a BRUKER DRX 600 spectrometer fitted with a BBO probe. Spectra were acquired with presaturation of the residual water resonance in the interscan delay. 256 FIDs consisting of 64K data points were acquired for each sample. Spectra were exported as ASCII-files for principal component analysis (PCA) of the differences in the spectral region from 4.70-0.5 ppm. The PCA analyses were done using the prcomp routine of the pls-package (Mevik and Wehrens, 2007) in R 2.5.0(R-project).

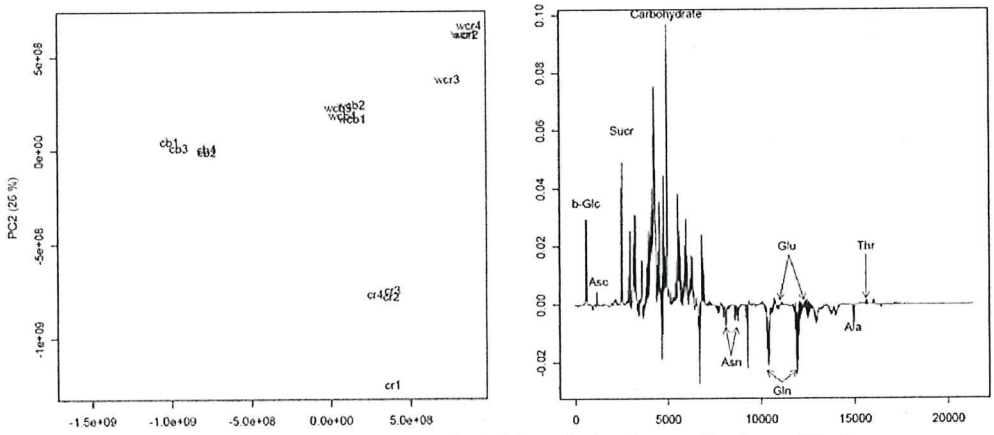

Figure 1: a) Scoreplot of PC1 vs PC2 from the PCA analysis, cb=genetically modified (gm) leaf, cr= gm root, wcb= wild type leaf, wcr =wild type root. b) loadingplot for PC1.

The scoreplot is presented in figure 1 and shows a clear clustering of all groups. The loadingplot of PC1 is presented in figure 2, and shows the major metabolites responsible for the variation in the PC1 direction. β-Glucose, ascorbate, sucrose, asparagines, glutamine, glutamate, alanine and threonine together with the carbohydrate region from 4.5-3 ppm were identified among the metabolites responsible for the separation of the groups. The underlying metabolic causes will be discussed.

References

Mevik, B.H., Wehrens, R., 2007. The pls package: Principal component and partial least squares regression in R. *J Stat Softw* Vol 18.

R-project, http://www.r-project.org/.

POSTER ABSTRACTS

Inherent molecular complexity of pelanin, a complex antiviral anthocyanin, resolved by natural abundance heteronuclear ^{1}H-^{1}H-^{13}C 3D NMR

Torgils Fossen*, Nils Åge Frøystein and Øyvind M. Andersen

Structural assignment of pelargonidin 3-*O*-[6-*O*-(4-*O*-*E*-*p*-coumaroyl-*O*-α-rhamnopyranosyl)-β-glucopyranoside]-5-*O*-β-glucopyranoside (pelanin) in acidified deuterated methanolic solution, performed by ^{1}H-^{1}H-^{13}C natural abundance 3D NMR spectroscopy, revealed that under these solution conditions pelanin occurred on two enantiomeric hemiketal equilibrium forms, in addition to the flavylium form. The relative proportions of the hemiketal equilibrium forms increased upon storage time. The overlap of some ^{1}H chemical shifts of the hemiketal anthocyanidins with ^{1}H chemical shifts of the *p*-coumaroyl unit of the main equilibrium form, namely the flavylium cation, which may have prevented their detection previously, was resolved in the 3D NMR spectra. High-quality ^{1}H-^{1}H-^{13}C natural abundance 3D HSQC-TOCSY spectrum of pelanin (sample concentration 60 mM) dissolved in acidified methanolic solution was recorded in 6 hours on a 600 MHz NMR instrument equipped with a cryogenic probe. Spectral analyses revealed evidence of inter- or intra-molecular self-association of the flavylium form.

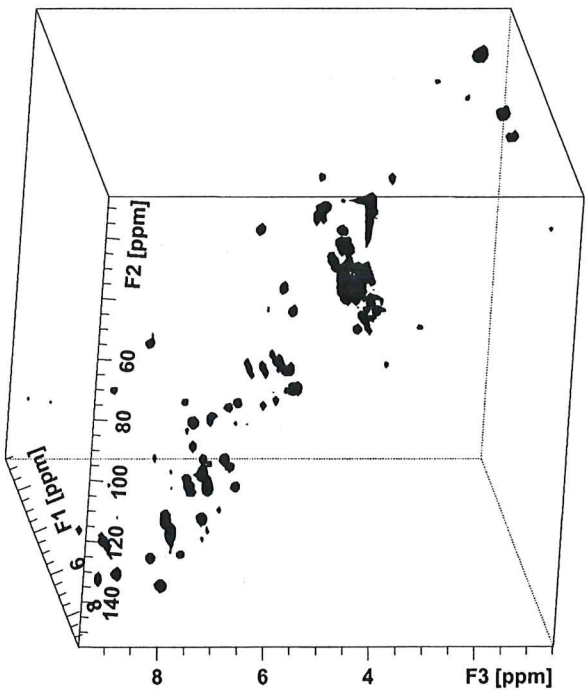

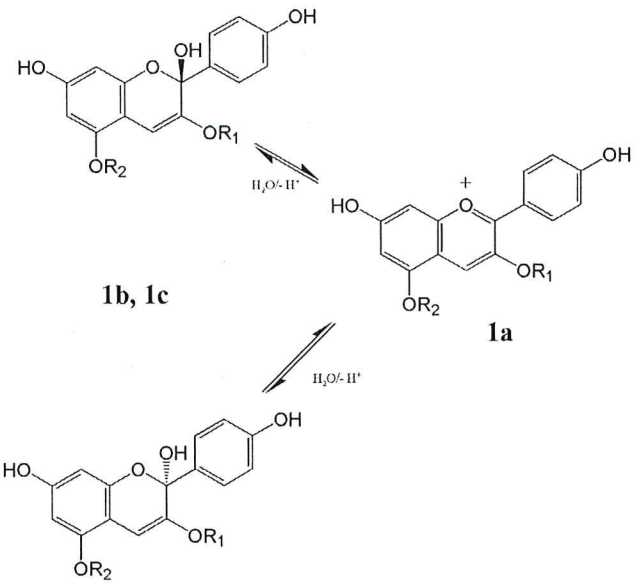

*Correspondence to: Torgils Fossen, Department of Chemistry, University of Bergen, Allégt. 41, N-5007 Bergen, Norway.
Email: Torgils.Fossen@kj.uib.no
Contract/grant sponsor: Norwegian Research Council

CHARACTERIZATION OF THE POROSITY IN MODIFIED MCM-22 BY ^{129}Xe NMR

A. van Miltenburg[1], J. Pawlesa[2], L.C. de Ménorval[3], A. M. Bouzga[1], M. Støcker[1], J. Čejka[2]

[1] *SINTEF Materials and Chemistry, Department of Hydrocarbon Process Chemistry, P.O. Box 124 Blindern, N-0314 Oslo, Norway*
Tel.: +47-22067957, fax: +47-22067350, e-mail: Arjen.vanMiltenburg@sintef.no

[2] *J. Heyrovský Institute of Physical Chemistry, Academy of Sciences of the Czech Republic, Dolejškova 3, CZ-182 23 Prague, Czech Republic*

[3] *Laboratoire des Matériaux Catalytiques et de Catalyse en Chimie Organique (UMR 5618 CNRS), ENSCM, 8 Rue de l'Ecole Normale, 34296 Montpellier Cédex 5, France*

Due to the slow diffusional transport through the small 10-ring pores in the layered zeolite crystal-slabs, the catalytic performance of MCM-22 is restricted. MCM-22 (IZA code MWW) consists of a two-dimensional microporous structure composed of two independent channel systems: a sinusoidal intralayer channel system and an interlayer system with 12-ring supercages.
In order to increase the intermolecular transport, the zeolite was modified using steam or alkaline post-synthesis treatment steps [1]. These treatments create additional porosity in the zeolite porestructure. Also they could connect the two 2-dimensional pore systems, allowing a faster transport of molecules perpendicular to the surface of the thin zeolite slabs.
In order to characterize the formation of this additional porosity, ^{129}Xe NMR was used. The NMR chemical shift of the ^{129}Xe atom (diameter 0.44 nm) is affected by the nearby zeolite structure in the narrow pores (≥ 0.41x0.51) of the (modified) zeolite. The chemical shifts (as a function of ^{129}Xe loading) can than be used to obtain information about the size of the various pores in the (modified) porous materials [2]. Furthermore, the ^{129}Xe atom has the advantage that it is inert for the zeolite framework and the results will therefore be representative for the materials.
The ^{129}Xe NMR analysis showed that already at a concentration of 0.05 mol NaOH l^{-1} additional pores are formed in the MCM-22 zeolite. Higher alkaline concentrations show a further development of the resonance corresponding to these additional pores. Furthermore, a decrease in the ^{129}Xe NMR resonance corresponding to the pores of the parent MCM-22 is observed. After an alkaline treatment with 0.50 mol NaOH l^{-1} a significant change in pore sizes was observed; the original pores are no longer visible in the ^{129}Xe NMR spectra, while new resonances (with corresponding poresizes) have appeared. These results were supported by other characterization techniques.

This research is financially supported by the Marie Curie Scholarship (INDENS: MRTN-CT-2004-005503)).

1 Pawlesa, J, Bejblov, M, Sommer, L, Bouzga, AM, Stöcker, M, Čejka, J, *Stud. Surf. Sci. Cat.* 170 (2007) 610-615.
2 Julbe, A., Farrusseng, D., de Ménorval, LC, Guizard, C, *Sep Purif Technol* 32 (2003) 165-173.

Determination of time-dependent diffusion, T_2 and water compartmentation in rat myocardium

T. Pavlin, P. Jynge, J. G. Seland

Department of Circulation and Medical Imaging, Norwegian University of Science and Technology, NO-7489 Trondheim, Norway

Introduction:
The aim of this work is to relate spatial and local mobility of water spins in rat myocardium by correlating time-dependent diffusion coefficient and T_2 relaxation constant. From spin mobility we attempt to infer the water compartmentation of rat myocardium which can help us to differentiate between healthy and diseased tissue. Due to the problems associated with heart motion, such correlation experiments have primarily been performed on other organs and systems [1-3]. We are able to perform the correlation experiments on viable myocardium by using isolated cardioplegic rat hearts.

Materials and Methods:
Five dissected rat hearts were perfused, alternatively, with regular and cardioplegic (20 mM of KCl) Krebs buffer solutions. NMR relaxography was performed *ex vivo* (Maran Ultra, Resonance Instruments Ltd, 23 MHz, 37°C). The flow of buffer solution was stopped during data acquisition. Time dependent diffusion-T2 correlations were measured using a combined Pulsed Gradient Stimulated Spin Echo-CPMG pulse sequence. The diffusion time varied from 5 ms to 80 ms. The diffusion encoding part of the sequence (PGSTE) employs a set of bipolar gradients (applied along the long-axis of the cardioplegic heart) which reduce the influence of eddy currents on the measured echoes in the CPMG train [4]. The heart rate was monitored throughout the experiment using software from AD Instruments.

Results and Conclusion:
The data reveals three T_2 components, with approximate values of 60 ms, 250 ms and 2200 ms, with different time-dependent diffusion characteristics which need to be investigated further. The component with longest T_2 is associated with water located on the surface of the heart, while the two remaining components most likely represent intra- and extra-cellular water. The diffusion data will give us information about the size and connectivity of the intra- and extra-cellular space.

References

1. Peled, S., et al., Magn Reson Med, 1999. 42(5): p. 911-918.
2. Windt, C.W., F.J. Vergeldt, and H. Van As, J Magn Reson, 2007. 185(2): p. 230-9.
3. Seland, J.G., et al., Phys Rev E Stat Nonlin Soft Matter Phys, 2004. 70(5 Pt 1): p. 051305.
4. Wu, D.H., A.D. Chen, and C.S. Johnson, Journal of Magnetic Resonance Series A, 1995. 115(2): p. 260-264.

Separating Signals from Intra- and Extracellular Water Compartments in Rat Skeletal Muscle *In Vivo* Using MEMRI

J. G. Seland[1], K. Helmer[2], G. Nair[2], D. G. Bennett[2], C. H. Sotak[2,3]

[1]Department of Circulation and Medical Imaging, Norwegian University of Science and Technology, Trondheim, Norway, [2]Department of Biomedical Engineering, Worcester Polytechnic Institute, Worcester, Massachusetts, United States, [3]Department of Radiology, University of Massachusetts Medical School, Worcester, Massachusetts, United States

Introduction. Tissue inter-compartmental equilibrium water exchange can significantly affect the quantitative analysis of various *in vivo* MR parameters. One method for investigating equilibrium-water-exchange effects is NMR Relaxography,[1] which can employ an MR contrast agent to selectively modify the T_1 relaxation time of one tissue compartment relative to the other. In the absence of a contrast agent, the inter-compartmental water exchange rate is significantly faster than the difference in longitudinal relaxation rates ($R_1 = 1/T_1$) in each compartment. In this case, a mono-exponential T_1 relaxation time would be measured. However, selective addition of an MR contrast agent (of sufficient concentration) to one compartment can increase the T_1-relaxation-rate difference between the two compartments (relative to the inter-compartmental exchange rate; which remains constant); potentially moving the system into an intermediate- or slow-exchange regime. If the slow-exchange regime can be achieved, then the MR signal contributions from each compartment can be separated on the basis of their T_1 relaxation time differences. In the simplest case, a bi-exponential T_1 relaxation time would be measured. One impediment to achieving the slow-exchange regime *in vivo* has been the difficulty in attaining the necessary contrast-agent concentration in one of the tissue compartments. In previous *in vivo* attempts in rat skeletal muscle using Gd(DTPA), only the intermediate-exchange regime could be achieved.[2] In this study, manganese-enhanced MRI (MEMRI) has been investigated as a method for separating and identifying the MR signals from intra- and extracellular water compartment in rat skeletal muscle *in vivo*.

Materials and Methods. The experiments were performed on a GE CSI-II 2.0T/45-cm imaging spectrometer operating at a ^{1}H frequency of 85.56 MHz. A 22 mm (ID), 4-turn solenoid RF coil was placed around the right thigh of male Sprague-Dawley rats. In order to prevent the RF field from extending outside the longitudinal edges of the coil, a doughnut-shaped piece of copper foil was placed at each end. This made it possible to perform localized spectroscopy using only the RF-field profile of the coil itself. $MnCl_2$ was infused through a catheter inserted in the femoral vein. Five rats, with an average weight of 320 g, were studied at six different [Mn^{2+}] (20, 30, 40, 50, 60 and 70 mM); each infused successively over periods of 32 min at a flow rate of 0.0266mL/min. The total accumulated dose was 0.715 mmol/kg Mn^{2+} after 192 min. During infusion, T_1 was measured over 6-min intervals using a standard Inversion Recovery (IR) pulse sequence with an adiabatic inversion pulse. The data were analyzed by Inverse Laplace Transform (ILT); which, when performed on the IR data, yields the distribution of T_1 relaxation times in the sample.[1]

Results. A typical series of T_1 distributions, as a function of infused [Mn^{2+}], over time is shown in the Figure (Exp. No 5). At low [Mn^{2+}] only one peak (located around 1170 ms) is observed. This is indicative of the fast-exchange regime, where the difference in the T_1 relaxation rates (ΔR_1) between the two compartments is small relative to the inter-compartmental equilibrium water exchange rate. However, as the administered [Mn^{2+}] increases over time, the mean of the single distribution shifts to lower T_1 values. At an infused [Mn^{2+}] = 50 mM, a second distribution appears. If there is no significant transport of Mn^{2+} into the skeletal-muscle intracellular (IC) space over the experimental time course, then the fast T_1 component can be assumed to arise from water in contact with Mn^{2+} in the extracellular (EC) space (as well as in equilibrium with the vascular water). The appearance of two T_1 distributions also heralds the onset of the slow-exchange regime. The means of the T_1 distributions (and the fractional population, p1, of the short-T_1 component; p2 = 1.0 – p1) at the highest (final) infused [Mn^{2+}] are given in the Table and were similar for all experiments. The fraction of the shortest component (p1) corresponds well to values for the skeletal muscle EC fraction reported in the literature.[3]

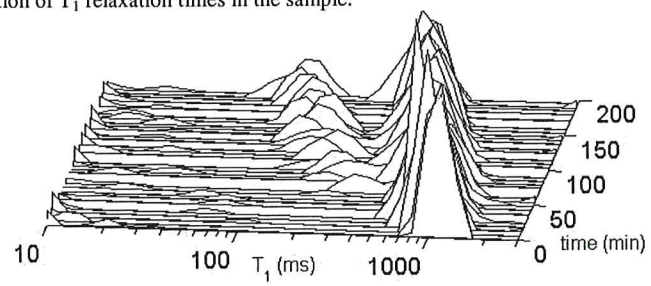

Exp. no	T_1 initial	T_1-1 final	T_1-2 final	p1 final
1	1197	134	539	0.25
2	1175	155	616	0.24
3	1230	138	530	0.27
4	1152	130	480	0.26
5	1170	95	473	0.24
Overall (SD)	1185 (30)	130 (22)	528 (57)	0.25 (0.01)

Discussion and Conclusions. A similar study using Gd(DTPA) was not able to separate the water signals from the two compartments in rat skeletal muscle.[2] A shoulder was observed at highest [Gd(DTPA)]; perhaps indicating the approach of the slow-exchange regime. In the Gd(DTPA) study, the shortest T_1 value attained was ~600 ms at the highest dose. In our study, a value of ~500 ms was observed at the onset of peak separation, with a value of ~350 ms reached at the highest [Mn^{2+}], indicating a significantly higher [Mn^{2+}] and/or relaxivity for Mn^{2+} the EC space. Mn^{2+} bound to macromolecules in the plasma and interstitial space can result in a 5-fold increase in relaxivity vs Mn^{2+} in water.[4] The enhanced relaxivity, in combination with [Mn^{2+}], appears to be sufficient to achieve the slow-exchange regime; allowing separation of the EC and IC water signals. By contrast, the relaxivity of Gd(DTPA) is the same in water and plasma,[3] which may explain why only the intermediate-exchange regime was attained in (2), even at plasma [Gd(DTPA)] as high as 10 mmol/L. The ability to differentiate between IC and EC water compartments *in vivo* using MEMRI would have important implications for studying inter-compartmental equilibrium water exchange in skeletal muscle under a variety of circumstances as well as other applications.

References. 1. Labadie C, *et al*, J. Magn. Reson. Ser B, 1994;105: 99-112.
2. Landis CS, *et al*, Magn. Reson. Med., 1999; 42: 467-478. 3. Donahue, KM, *et al*, Magn. Reson. Med., 1995; 34: 423-432.
4. Wendland, MF, NMR Biomed., 2004; 71: 581-594.

□

Isolation and characterization of macro cyclic peptides

Lars Skjeldal

Department of Chemistry, Biotechnology and Food Science
Norwegian University of Life Sciences

☐ preferred ORAL presentation ☒ POSTER presentation

Rapid Determination of the Fat Content in Packaged Dairy Products by Unilateral NMR

E. Veliyulin[1], I.V. Mastikhin[2], A.E. Marble[2] and B.J. Balcom[2]

[1] SINTEF Fisheries and Aquaculture, N-7465 Trondheim, Norway
[2] MRI Centre, Department of Physics, University of New Brunswick, Fredericton, NB, Canada E3B 5A3

Abstract:
Knowledge of the fat content in dairy products is important for both industry and consumers. A new procedure for rapid and non-destructive determination of the fat content in dairy products in commercial packages using a unilateral NMR was proposed. Rapid accumulation of the NMR signal was achieved by the use of a newly developed unilateral magnet array with a well-controlled magnetic field and optimized for sensitivity [1]. The sample magnetization was prepared using either T_1 suppression or diffusion editing and read out via a CPMG pulse sequence (Fig.1). A linear correlation between the measured NMR signal from the fat component and the declared fat content in the tested products validated both approaches as viable instrumental methods. The shortest measurement time was about 7 s.

Advantages of the unilateral NMR method, including hardware simplicity and accommodation of commercially packaged products make it attractive for routine use in industry.

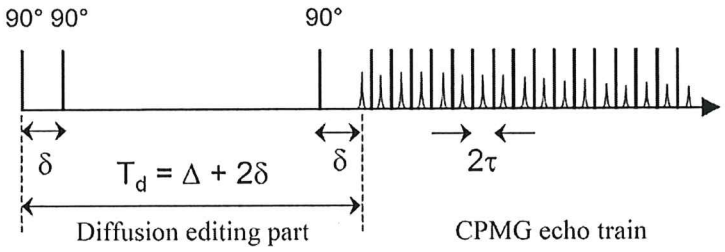

Fig.1: Diffusion edited CPMG pulse sequence [2] effectively suppressing the contribution of the water component in the dairy products

1. Marble, A.E., Mastikhin, I.V., Colpitts, B.G., Balcom, B.J., A compact permanent magnet array with a remote homogeneous field. *J Magn Reson* **186** (2007) 100-104.

2. Rata, D.G., Casanova, F., Perlo, J., Demco, D.E. and Blümich, B., Self-diffusion measurements by a mobile single-sided NMR sensor with improved magnetic field gradient, *J Magn Reson* **180** (2006) 229-235.

☐ preferred ORAL presentation ☒ POSTER presentation

Rapid Determination of the Moisture Content in Wood Shavings Using Time Domain NMR

E. Veliyulin[1], I.V. Mastikhin[2], A.E. Marble[2], G.M. Jenkins[3]and B.J. Balcom[2]

[1] SINTEF Fisheries and Aquaculture, N-7465 Trondheim, Norway
[2] MRI Centre, Department of Physics, University of New Brunswick, Fredericton, NB, Canada E3B 5A3
[3] Wood Science and Technology Centre, Faculty of Forestry and Environmental Management, University of New Brunswick, Fredericton, NB, Canada E3C 2G6

Abstract:
A new procedure of rapid and non-destructive determination of the moisture content in wood shavings based on time domain NMR is proposed. The solid echo NMR technique [1] was implemented in the on board NMR analyzer (Bruker the minispec mq10), allowing information concerning rapidly relaxing hydrogen atoms from the cellulose, as well as from the hydrogen in the water phase, to be obtained.

Linear correlation (Fig.1) between the latter component and the gravimetrically determined moisture content in the tested samples has been observed. Speed and simplicity of the time domain NMR method make it attractive for routine use in the wood industry.

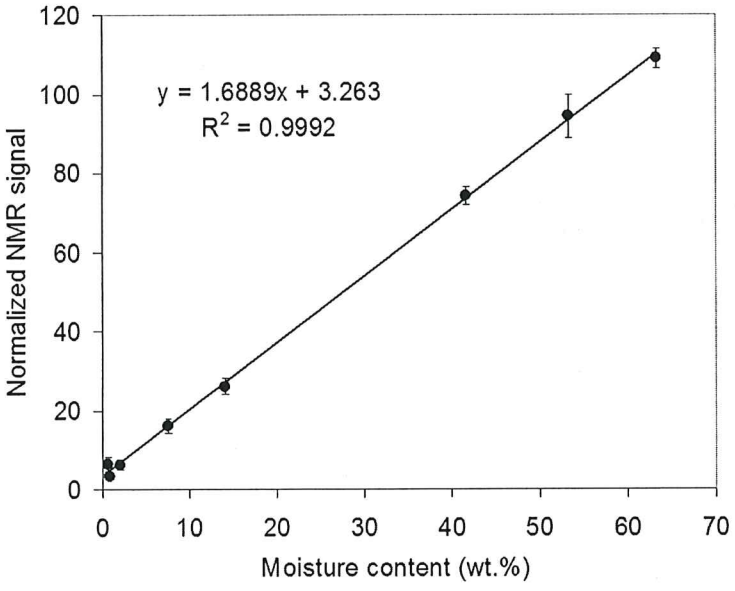

Fig.1: NMR signal from the shaving samples normalized with sample weight as a function of the gravimetrically determined moisture content

1. Slichter, C.P. 1990. Principles of Magnetic Resonance, Springer-Verlag, New-York, pp. 371-379.

List of participants

	Name	Email	Affiliation
1.	Aachmann, Finn	finn.aachmann@biotech.ntnu.no	NTNU
2.	Argyropoulos. Dimitris	Dimitris.Argyropoulos@varianinc.com	VARIAN Limited
3.	Arnott, Richard	richard.arnott@varianinc.com	VARIAN Limited
4.	Aursand, Marit	Marit.Aursand@sintef.no	SINTEF
5.	Berntsen, Andreas N.	Andreas.Berntsen@iku.sintef.no	SINTEF
6.	Bjerkeseth, Leif Haldor	Leif-Haldor.Bjerkeseth@ffi.no	FFI
7.	Bouzga, Aud M	Aud.Mjarum.Bouzga@sintef.no	SINTEF
8.	Dikiy, Alexander	alex.dikiy@biotech.ntnu.no	NTNU
9.	Einarsson, Larus	larus.einarsson@bruker.se	Bruker Biospin
10.	Fletcher, Mark	mark.fletcher@varianinc.com	VARIAN Limited
11.	Frøystein, Nils Åge	Nils.Froystein@kj.uib.no	University of Bergen
12.	Gran, Hans Christian	Hans-Christian.Gran@ffi.no	FFI
13.	Grasdalen, Hans	hans.grasdalen@biotech.ntnu.no	NTNU
14.	Gribbestad, Ingrid	ingrid.s.gribbestad@ntnu.no	NTNU
15.	Hansen, Eddy Walther	e.w.hansen@kjemi.uio.no	University of Oslo
16.	Haraldseth, Olav	olav.haraldseth@ntnu.no	NTNU
17.	Jensen, Magnus	Magnus.Jensen@kj.uib.no	University of Bergen
18.	Karlsson, Göran	goran.karlsson@nmr.gu.se	Göteborg University
19.	Kryczka, Tomasz	tomasz.kryczka@ntnu.no	NTNU
20.	Mair, Ross	rmair@cfa.harvard.edu	Harvard-Smithsonian CfA
21.	Melø, Torun Margareta	Torun.Melo@ntnu.no	NTNU
22.	Nerdal, Willy	Willy.Nerdal@kj.uib.no	University of Bergen
23.	Pavlin, Tina	tina.pavlin@ntnu.no	NTNU
24.	Petersen, Dirk	dirk.petersen@kjemi.uio.no	University of Oslo
25.	Risa, Øystein	oystein.risa@ntnu.no	NTNU
26.	Rise, Frode	frode.rise@kjemi.uio.no	University of Oslo
27.	Sandström, Dick	dick.sandstrom@bruker.se	Bruker Biospin
28.	Seland, John Georg	john.seland@ntnu.no	NTNU
29.	Simic, Nebojsa	simic@chem.ntnu.no	NTNU
30.	Sitter, Beathe	beathe.sitter@ntnu.no	NTNU
31.	Skjeldal, Lars	larssk@umb.no	Norwegian University of Life Sciences
32.	Sletten, Einar	Einar.Sletten@kj.uib.no	University of Bergen
33.	Solli Sal, Lena	lenaso@nt.ntnu.no	NTNU
34.	Steinkopf, Signe	sst@hib.no	Bergen University College
35.	Stepišnik, Janez	janez.stepisnik@fmf.uni-lj.si	University of Ljubljana
36.	Størseth, Trond	Trond.R.Storseth@sintef.no	SINTEF
37.	Taylor, Richard	Richard.taylor@ewos.com	Ewos Innovation
38.	Tessem, May-Britt	may-britt.tessem@ntnu.no	NTNU
39.	Thuen, Marte	marte.thuen@ntnu.no	NTNU
40.	Tønsager, Janne	Janne.Tonsager@ffi.no	FFI
41.	Ukkelberg, Åsmund	asmund.ukkelberg@kjemi.uio.no	University of Oslo
42.	van Miltenburg, Arjen	Arjen.vanMiltenburg@sintef.no	SINTEF
43.	Veliyulin, Emil	Emil.Veliyulin@sintef.no	SINTEF
44.	Washburn, Kate	mondhaut@gmail.com	Victoria University of Wellington
45.	Zhang, Lili,	Zhang.Lili@kjemi.uio.no	University of Oslo